Heliyon 10 (2024) e28313

Contents lists available at ScienceDirect

Heliyon

journal homepage: www.cell.com/heliyon

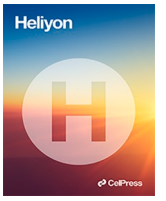

Research article

Thermal and structural characteristics of date-pits as digested by *Trichoderma reesei*

Samar Mohammed Khalaf Al-Saidi [a], Zahra Sulaiman Nasser Al-Kharousi [a], Mohammad Shafiur Rahman [a,*], Nallusamy Sivakumar [b], Hafiz Ansar Rasul Suleria [c], Muthupandian Ashokkumar [d], Malik Hussain [e], Nasser Al-Habsi [a]

[a] *Department of Food Science and Nutrition, College of Agricultural and Marine Sciences, Sultan Qaboos University, P. O. Box 34-123, Al-Khod 123, Oman*
[b] *Department of Biology, College of Science, Sultan Qaboos University, P. O. Box 34-123, Al-Khod 123, Oman*
[c] *School of Agriculture, Food and Ecosystem Sciences, Faculty of Science, The University of Melbourne, Parkville, VIC 3010, Australia*
[d] *School of Chemistry, The University of Melbourne, Australia*
[e] *School of Science, Western Sydney University, Australia*

ARTICLE INFO

Keywords:
Amorphous
Crystallinity
Glass transition
Hygroscopicity
Melting
Proton mobility
Trichoderma reesei

ABSTRACT

The objective of this study was to develop functional date-pits by mold digestion for the potential use in food products. Whole date-pits (WDP) and defatted date-pits (DDP) were digested by mold *Trichoderma reesei* at 20 °C. *T. reesei* consumed date-pits as nutrients for their growth, and DDP showed higher growth of molds as compared to the WDP. The mold digested WDP and DDP samples showed an increased water solubility and hygroscopicity as compared to the samples prepared by autoclaved. This indicated that the mold digestion transformed date-pits to hydrophilic characteristics. Thermal analysis indicated a structural change at −3.2 °C for the untreated WDP and it was followed by a glass transition shift (i.e. onset: 138 °C and a specific heat change: 295 J/kg °C), and an endothermic peak at 196 °C with enthalpy of 68 J/g for the solids melting-decomposition. Similar characteristics were also observed for treated samples with the two glass transitions. The total specific heat changes for WDP, autoclaved-WDP, and digested-WDP were observed as 295, 367, and 328 J/kg °C, respectively. The total specific heat changes for DDP, autoclaved-DDP, and digested-DDP were observed as 778, 1329, and 1877 J/kg °C, respectively. This indicated that mold digestion transformed more amorphous fraction in the DDP. The energy absorption intensities of the Fourier Transform Infrared (FTIR) spectra for the selected functional groups decreased by the mold digestion.

1. Introduction

Date-pits are by-products of date-processing factories and these contain a high amount of indigestible carbohydrates (i.e. fibers). The utilization of these by-products could have positively contributed to the circular economy and environmental sustainability. In the future, utilization of food waste and conventional inedible components could contribute a role in achieving food security. Many research works are now reported in developing food ingredients utilizing conventional inedible parts, such as skin, seeds, and hard

* Corresponding author.
E-mail address: shafiur@squ.edu.om (M.S. Rahman).

https://doi.org/10.1016/j.heliyon.2024.e28313
Received 8 November 2023; Received in revised form 12 March 2024; Accepted 15 March 2024
Available online 16 March 2024

leafy parts. However, these ingredients are difficult to add as to their original state because of their effects on the texture and sensory perceptions of formulated foods. Therefore, mechanical, chemical and microbial treatments are necessary to apply for making their suitability to be used in food products.

Date-pits need to be pre-treated to break down the lignocellulosic biomass and enhance their functionality for proper utilization [1]. Date-pits represent about 10–15% of the total date fruit mass and it depends on the variety [2]. Date-pits are considered as odorless with a light to dark brown color. Their taste are bland with little bitterness depending on the varieties [3]. Date processing plants usually discard many tons of date-pits that have a high amount of indigestible carbohydrates and these are rich in fibers [4]. Many investigations reported the chemical composition of date-pits, which varies depending on the date variety. Hossain et al. [5] reported the chemical composition of 23 date-pits varieties. According to their study, carbohydrate content ranged from 70.9 to 86.9 g/100 g, oil content varied from 5.0 to 12.5 g/100 g, protein content ranged from 2.3 to 6.9 g/100 g, moisture content varied from 3.1 to 12.5 g/100 g and ash content ranged from 0.91 to 1.20 g/100 g. Date-pits are also rich sources of some vitamins, phytochemicals and minerals.

Date-pits are now utilized as an alternative feed for animal and in poultry industries [6]. The oil extracted from date-pits can be utilized as an edible oil for the production of food products, such as mayonnaise and for cosmetic and pharmaceutical purposes [7]. The dietary fiber of date-pits can be used in the production of fiber-based products including cake, fiber supplements, biscuits and breads. Therefore, date-pits fiber is a good substitute of wheat bran [8]. In addition, roasted date-pits can be used to produce a natural caffeine-free drink in the Middle Eastern region, which could offer a popular alternative to normal coffee [9]. Several studies on date-pits have discussed their biological and pharmacological properties of date-pits. Date-pits extracts exhibited antimicrobial and antiviral activities against different types of bacteria [10,11]. The high content of phenolic compounds and this can be used in the production of antioxidant supplements [12,13] Date-pits also showed the anti-inflammatory activity [5,14,15], anti-cancer [16], and anti-diabetic properties [17].

Date-pits are a rich source of dietary fiber [7]. The cellulose, hemicellulose and lignin contents in date-pits are 42.5, 17.5 and 11.0%, respectively [18]. Plant wastes are difficult to degrade and metabolize due to materials complexity. Negligible works on the digestion of date-pits are reported although the degradation of plant waste by microbial digestion is known [19]. There is ongoing research interest to investigate different cellulolytic enzyme for bioconversion of lignocellulosic substrates [20]. Cellulolytic organisms can break down the lignocellulosic biomass including cellulose, hemicellulose and lignin to produce desired chemicals and it would be otherwise difficult to utilize without digestion [21]. *Trichoderma reesei* is one of the main molds, which is commercially available to produce cellulases. This mold has the ability to degrade the cell wall polysaccharides of the plant, such as cellulose, hemicellulose and can produce great quantities of cellulolytic enzymes [22]. Alyileili et al. [23] studied the effects of degraded date-pits by *Trichoderma reesei* on the intestinal microbiota and growth performance of broilers. They used 10% degraded date-pits in broilers' diet and observed prebiotic effect by boosting gut health as evidenced from the bacterial population.

Thermal properties of foods are important to determine their processing conditions as well as stability during storage. Thermal analysis is a dynamic technique used to determine the physical state of foods. It is also used to recognize glass transition temperature, melting temperature, crystallization temperature, un-freezable water content and maximal-freeze-concentration conditions [24,25]. The differential scanning calorimetry (DSC) is a commonly used method for thermal analysis, when any state or phase change during heating or cooling can be determined [26]. Al-Mawali et al. [27] studied the thermal characteristic of untreated and alkaline treated date-pits powder (X_w: 8.8 g/100 g sample) by DSC. Functional groups and proton mobility of date-pits can be used to determine their molecular interactions and structural behavior. Low Field Nuclear Magnetic Resonance (LF-NMR) determines various pools of protons in foods like T_{2b} (rigid or strongly bound protons), T_{21} (semi-rigid or moderately bound protons) and T_{22} (mobile or weakly bound protons) relaxation times [28,29]. Fourier transform infrared (FTIR) spectroscopy is a technique used to determine the behavior of functional groups and chemical compositions of a material [30].

Most literature focused on the pretreatments of the lignocellulosic biomass using mechanical (i.e., milling and grinding), chemical (i.e., alkali and acids), and physical (i.e., thermal, pressure and microwave) treatments. However, limited scientific research and literature is available on the microbial digestion of date-pits. The main objective of this study was to determine the effect of *T. reesei* on whole and defatted date-pits at high moisture digestion. In this study, whole and defatted date-pits were used since oil can affect the growth of molds. The physico-chemical, thermal (i.e. Differential Scanning Calorimetry, DSC) and molecular properties were measured to determine proton mobility (i.e. LF-NMR) and functional groups (Fourier Transform Infrared, FTIR). Mold digestion could produce modified date-pits fibers with improved functionality in relation to high amorphous fractions, and digested fractions could be suitable to be used in foods and fillers in bio-composite.

2. Materials and methods

2.1. Preparation of whole and defatted date-pits powder

Khalas varieties of date-pits were obtained from Nizwa Dates Factory, Oman. Date-pits were soaked in water for 2 h and these were washed with tap water to remove any adhering date flesh. These were then dried in a hot air drying oven (Gallenkamp, UK; model: 300 plus series) at 60 °C for 72 h. After drying, date-pits were cooled to 20 °C and ground into powder by a hammer mill (Model NO: Comotec 1090, Foss, Hoganas, Sweden). Particle size analysis was performed by passing the powder through 1–2 mm screens and stored in a bottle at 20 °C until used for analysis. Powdered date-pits were treated with petroleum ether to remove oil (CAS number: 8032-32-4) using a soxhlet apparatus. The ratio of date-pits and petroleum was at 2:10 (g:ml), and 8 h extraction time was used. The defatted date-pits were dried in an oven at 60 °C for 18 h and then stored in a bottle at 20 °C.

2.2. Preparation of Trichoderma reesei spore suspension

T. reesei spore suspension was prepared using the method of Chaiwut et al. [31]. *T. reesei* (ATCC 26921) was purchased from the American Type Culture Collection as a freeze-dried culture in an ampoule. The ampoule was opened and dried culture was rehydrated following the methods as described by the manufacturer (i.e. 1.0 ml of sterile distilled water was added to the pellet and it was then stirred to form suspension). A subsample was transferred from the rehydrated *T. reesei* culture using a sterile loop to Potato Dextrose Agar (PDA) (CAS number 9002-18-0492-62-6) plates, which were prepared as guided by the manufacturer (Oxoid, UK). After inoculation, the PDA plates were incubated (Gallenkamp, UK) at 25 °C for 7 days. It was then transformed to yellow-green pigmented visible colonies. The culture of *T. reesei* was maintained on PDA agar slants. *T. reesei* spore suspension was prepared by transferring the colonies of *T. reesei* into 50 ml of sterile distilled water using a sterile loop. It was then mixed vigorously using a vortex (Scilogex, MX-S, Rocky Hill, US). The initial concentration of spores was adjusted using a hemocytometer to 5×10^6 spore/ml.

2.3. Microbiological digestion of date-pits using T. Reesi

The WDP and DDP were prepared by adding 10% of whole date-pits into 90 ml of distilled water in glass bottles (untreated sample, UNT). The controls were then sterilized in an autoclave (TOMY, SX-500E, HANYO) at 121 °C for 15 min (autoclaved sample, AUT). Following sterilization, the controls were incubated (Gallenkamp, UK) at 25 °C with shaking at 160 rpm for 2 months in the case of whole date-pits samples and 4 months in case of defatted date-pits. Two batches of samples (i.e. WDP and DDP) were prepared the same way as control. After sterilization, 2% of *T. reesei* spore suspension was added to the whole and defatted date-pits samples. The samples were incubated in a shaker similarly to the control (digested sample, DNR).

2.4. Growth of Trichoderma reesei by visible count

The count of *T. reesei* colonies was performed every week using spread plate method and PDA medium as described by Hassan et al. [32]. In order to count the *T. reesei* colonies, serial dilutions were prepared to dilute the samples. For the first dilution, a sterile pipette was used to transfer 1 ml of the sample to a tube holding 9 ml of Maximum Recovery Diluent (MRD) (CB number CB7355314) (Oxoid, UK). Then, the content of the tube was mixed using a vortex (SCILOGEX, MX-S). After mixing, 0.1 ml was transferred to PDA dishes and spread using a sterile spreader. For second dilution, 1 ml was transferred from the first tube to a second tube containing 9 ml of MRD and this process was repeated until all dilutions (10^{-1} to 10^{-7}) were prepared. The PDA dishes were kept in the incubator (Gallenkamp, UK) at 25 °C for two days. Three plates were prepared from each dilution. The colonies were counted by a colony counter and the population number of *T. reesei* was determined using the following Equation (1):

$$Number\ of\ Mold = \frac{\text{Average number of colonies on plate} \times \text{Dilution showing growth}}{\text{Volume of sample}} \quad (1)$$

2.5. Microscopic examination

The growth of *T. reesei* was examined using a method described by Carpa et al. (2014). A drop of each sample (i.e. digested whole and defatted date-pits samples) was added on a clean slide using a sterile loop. Then, a drop of lactophenol cotton blue dye (CAS number 56-81-5) was mixed with the drop of sample to visualize the growth of molds. The slides were finally fixed under the microscope to observe the growth of *T. reesei* using different magnifications and to compare the differences between the controls and samples.

2.6. Drying process and moisture content

The treated date-pits samples and controls were placed in glass dishes and dried using hot air drying in an oven (Binder, USA) at 65 °C for 48 h. Initial moisture content was determined gravimetrically using the standard method of the Association of Official Analytical Chemists [33]. After drying, samples were equilibrated at relative humidity of 11.1% (i.e. water activity of 0.111). In order to measure moisture content of the sample, about 0.5 g of each sample was weighed in a dried pre-weighed aluminum dish in duplicate and dried in a hot air oven (Gallenkamp, England) at 105 °C for 18 h and the initial and final mass of the sample were used to measure moisture content.

2.7. Water absorption and water solubility

Water absorption and solubility were determined by centrifugation as described by Cadavid et al. [34]. Sample (0.5 g) was weighed in a centrifuge tube and soaked in 5 ml of distilled water for 30 min at room temperature. After soaking, samples were centrifuged at 4000 rpm for 10 min using a centrifuge machine (Harrier 18/80, CA, UK). The supernatant was separated by draining liquid in a pre-weighed beaker and initial weight was recorded. The initial weight of pellet was taken by weighing pellet in a pre-weighed centrifuge tube and then removed in a pre-weighed beaker. The supernatant and pellet were dried in a hot air oven (Gallenkamp, England) at 105 °C for 18 h and final weights were taken. The water absorption (Equation (2)) and water solubility (Equation (3)) were calculated from the following equations:

$$Water\ absorption = \frac{\text{Final weight of pellet} - \text{Initial weight of pellet}}{\text{Initial weight of pellet}} \quad (2)$$

$$Solubility = \frac{\text{Final mass of dry matter}}{\text{Initial total mass of supernatant}} \quad (3)$$

2.8. Hygroscopicity

Hygroscopicity was measured by equilibrating the WDP and DDP samples in a controlled humidity chamber (Model 240, Binder, NY, USA) as described by Al-Khalili et al. [35]. Each ample (0.2 g) was weighed in an aluminum dish in triplicate and placed in a humidity chamber at 30 °C and 90% relative humidity. The samples were equilibrated for 2.5 h and hygroscopicity was determined form the moisture content.

2.9. Low Field Nuclear Magnetic Resonance (LF-NMR)

Proton mobility of whole and defatted date-pits was determined using the protocol as described by Al-Habsi et al. [28]. A Bruker Minispec MQ20 NMR analyzer (20 MHz, Karlsruhe, Germany) was used. The spin-spin relaxation time T_2 of proton was measured with Carr-Purcell-Meiboom-Gill pulse sequence. The NMR signal was set at 90° pulse followed by a train of 180° pulses and the pulse separating was set to 0.04 ms. The recorded free induction decay (FID) signal was analyzed using tri-exponential function as (Equation (4)):

$$\frac{S_2}{S_{2,0}} = I_{2b}\exp\left(-\frac{t}{T_{2b}}\right) + I_{21}\exp\left(-\frac{t}{T_{21}}\right) + I_{22}\exp\left(-\frac{t}{T_{22}}\right) \quad (4)$$

where $S_{2,0}$ and S_2 are the intensities at zero and any time, respectively for T_2 relaxation, I_{2b}, I_{21}, and I_{22} are the first, second, and third linear regions of T_2 relaxation curve (i.e., pre-exponential factors) and T_{2b}, T_{21}, and T_{22} are the relaxation times for rigid, semi-rigid, and mobile pools of protons, respectively. The number of segments were determined by the graphical method. In this method, numbers of linear portions of the plot ln ($S_2/S_{2,0}$) *versus* time were used rather than presuming segmentations. The intensities and relaxation times of rigid, semi-rigid, and mobile pools of protons were determined from the slopes and intercepts of these three linear segments. Six replicates were used for each sample. Three standards provided by the manufacturer with different concentrations were used to calibrate the LF-NMR. The ground date-pits samples were packed into a 10-mm NMR tube up to 3 cm height. First, the gain, number of scans, and duration of the relaxation were optimized. The scan number was used as 32 and the gain was ranged from 70 to 76 in order to maintain the initial intensity of around 80% in all samples.

2.10. Differential scanning calorimetry (DSC)

Thermal properties including structural relaxation, glass transitions, solids melting-decomposition were measured by a differential scanning calorimetry (DSC Q10, TA Instruments, New Castle, DE, USA). German Society of Thermal Analysis (GEFTA) protocol was used for temperature calibration. DSC was calibrated using distilled water (melting point 0 °C; ΔH_m 334 J/g), and indium (melting point 156.5 °C; ΔH_m 28.5 J/g) for heat flow and temperature. A sample of 3–5 mg was placed in a Tzero hermetic aluminium pan and sealed with a lid [27]. Empty sealed pan was used as a reference and nitrogen was used as a carrier gas for the DSC at a flow rate of 50 ml/min. The aluminium pan with sample was placed on the DSC heating plate, and it was cooled to −90 °C at 5 °C/min and it was then equilibrated for 3 min. Following equilibration, the sample was scanned from −90 °C to 300 °C at a rate of 10 °C/min. DSC thermogram was analyzed for structural change, glass transition, exothermic increase and solids melting-decomposition peak. The glass transition was identified by a vertical shift in the heat flow curve. Solids melting-decomposition was identified by an endothermic peak and an exothermic increase was considered as cold crystallization or molecular ordering. Any change in slope was considered as structural change in the sample. In the DSC measurement, each sample was replicated three to four times.

2.11. Fourier Transform Infrared (FTIR) spectroscopy

Functional groups of whole and defatted date-pits were determined using FTIR Spectrometer (Bruker, Germany) and it was based on the method as described by Nabili et al. [36]. A sample (0.02 g) was added to 2 g of potassium bromide (KBr) and mixed together using an agate mortar. Then, 0.2 g of the mixture was transferred to a die and the die was then compressed in a hydraulic press (Specac, Brilliant Spectroscopy, 15T) by applying a pressure of 10 tons for 7 min. It was then transformed to pellets (discs), which were used in determining FTIR spectra. The diameter of the sample was 13 mm. All spectra were obtained from 32 scans at a resolution of 4 cm^{-1}. FTIR spectra were collected in the IR absorbance range from 4000 to 400 cm^{-1}. FTIR spectrum was calibrated with room air. The characteristic peaks of each spectrum at specific locations (i.e. wave number and absorption intensity) was analyzed. The measurement was replicated 9 times (i.e. 3 measurements from 3 tablets) and then spectra were averaged.

2.12. Statistical analysis

Values were presented as average and expanded uncertainty at 0.95 confidence. ANOVA and LSD were performed using ezANOVA. The linearity of the segments was determined with Microsoft Excel [37]. The value of R^2 was used as a goodness-of-fit. Significant difference was considered when a p-value was less than 0.05.

3. Results and DISCUSSION

3.1. Microbiological digestion and growth of mold in whole and defatted date-pits

The moisture contents of the whole and defatted date-pits were 2.5 ± 0.3 and 3.3 ± 0.4 g/100 g sample, respectively. Fig. 1 shows the growth curve of *T. reesei* in treated whole (Fig. 1A) and defatted date-pits (Fig. 1B) (i.e. WDP and DDP). It shows four phases (i.e. lag, exponential, stationary, and death). In the case of WDP, the lag phase was observed up to 3 days followed by the log phase until 35 days. The stationary phase ended at 42 days and then started the death phase. The growth curve shows that *T. reeesi* used date-pits as nutrients for their growth. In the case of DDP, the death phase started at 64 days, whereas in whole date-pits it started at 42 days. This indicated that defatted date-pits supported better growth of the mold as compared to the whole date-pits ($P < 0.01$). Similarly, Altieri et al. [38] observed that the fatty acids (i.e. lauric, myristic, and palmitic acids) inhibited the growth of *Aspergillus* spp. and *Penicillium* spp. by prolonging the minimum detection time and the lag time. Likewise, Krisch et al. [39] observed that essential oils and their components reduced or stopped the growth of molds. These essential oils also decreased the cell growth in the stationary phase. Photographs of the untreated and treated whole-date-pits powder are shown in Fig. 1. The particles of the autoclaved (Fig. 1D) and mold digested (Fig. 1E) whole date-pits showed much smaller size as compared to the untreated date-pits (Fig. 1C). In addition, digested date-pits (Fig. 1E) shows much darker color as compared to the autoclaved and untreated whole date-pits. This could be due to the release of bound lignin within the date-pits matrix. Munoz-Tebar et al. [1] identified that lower particle size of date-pits flour showed higher level of polyphenols and antioxidant capacity. Therefore, lower particle size of the digested date-pits could increase their functionality.

3.2. Growth of mold and their Morphology during digestion

Fig. 2 shows the optical microscopic views of autoclaved and digested whole and defatted date-pits. In the case of autoclaved whole date-pits, oil droplets and date-pits solids were observed (Fig. 2A). Fig. 2B shows the presence of spores and hyphae of *T. reesei* between the date-pits particles. This indicated that molds were actively growing and proliferating using the date-pits as a source of their

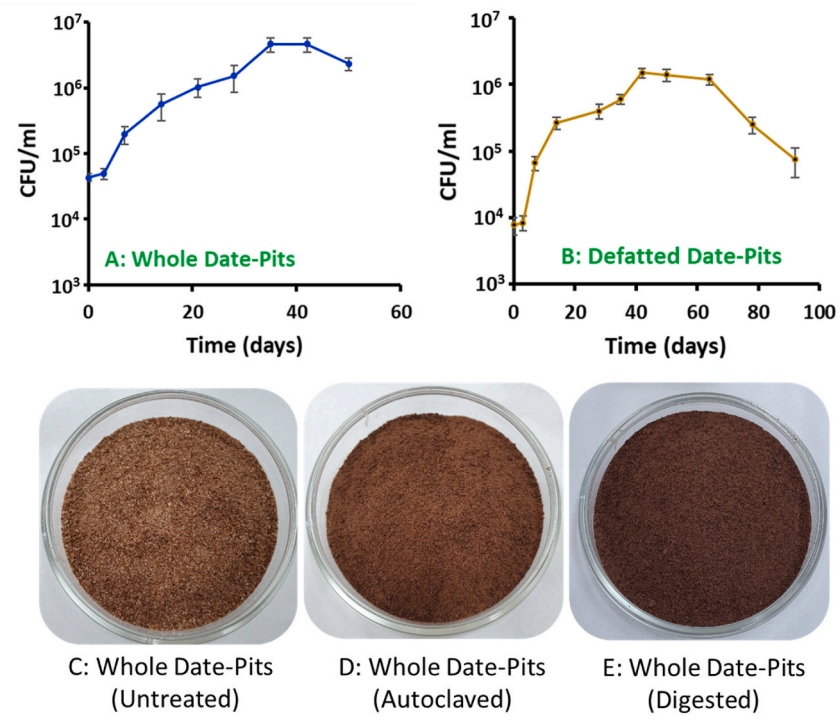

Fig. 1. Mold growth as a function of mold digestion time (A: Whole date-pits, WDP), B: Defatted date-pits, DDP), and photographs of the whole date-pits (C: untreated, D: autoclaved and E: digested).

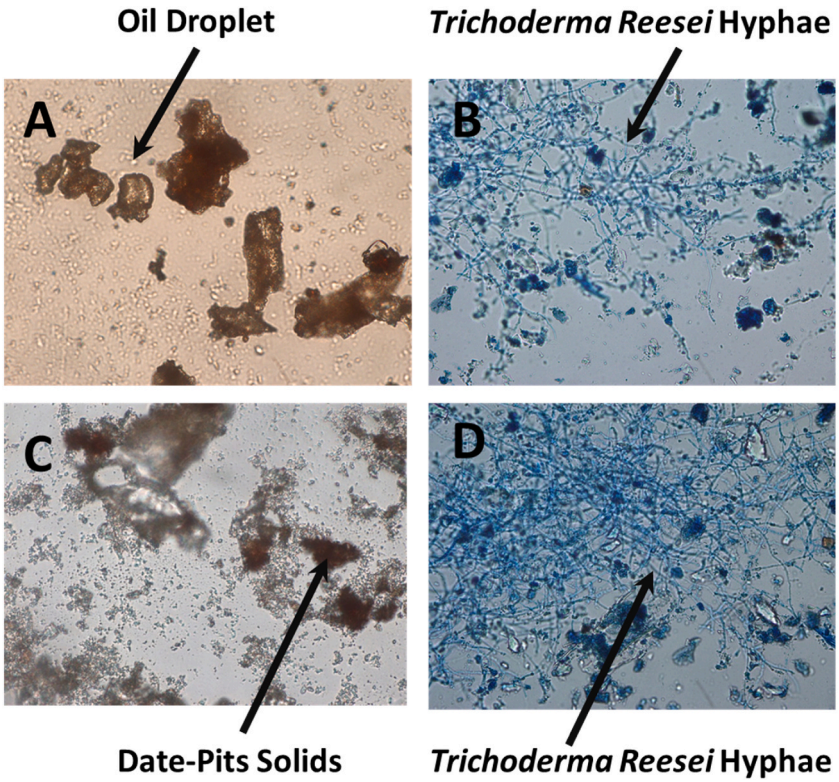

Fig. 2. Optical microscopy of autoclaved and digested date-pits with mold, A: Autoclaved whole date-pits (control), B: Digested whole Date-Pits, C: Autoclaved defatted date-pits, D: Digested defatted date-pits.

nutrients. However, oil droplets could not be observed after digestion with mold (Fig. 2B). In addition, the digested powder was more sticky (manually evaluated) as compared to the autoclaved date-pits (control). Defatted date-pits showed only water and solids phases without oil phase (Fig. 2C). Similar growth of spores and hyphae of *T. reesei* were observed in the case of digested defatted date-pits (Fig. 2D). Alyileili et al. [40] studied the degradation of fresh date-pits by *T. reesei* considering solid-state degradation (SSD) and observed that degraded date-pits improved the antioxidant responses and biochemical parameters of broiler chickens, when treated date-pits were added in their feeds. It was observed that degraded date-pits by *T. reesei* promoted the gut microbiota of broilers. They observed a lower total bacterial count as well as a reduced number of *Salmonella* spp., *Campylobacter* spp., *Shigella* spp., and *Escherichia coli*. In addition, degraded date-pits showed prebiotic effect, improved growth performance and similar performance as antibiotics used in diet [23]. This could be due to the release of bound bioactive compounds or molds could generate bioactive compounds.

3.3. Physico-chemical properties of whole date-pits powder

Moisture content (X_w), solubility, water absorption, and hygroscopicity (HY) of whole and defatted date-pits are presented in Table 1. The solubility of untreated WDP was 1.3 g/L, while it shifted to 1.0 g/L in the case of autoclaved treatment ($P < 0.05$). Cadavid et al. [34] found water solubility of asparagus fiber ranged from 1.1 to 1.6 g/L and it was ranged from 0.4 to 0.7 g/L in commercial corn flour [40]. This difference could be due to the structural modifications taking place during fibre grinding (i.e. reduced particle size was exposed to a larger surface area and surrounded by water [41]. In the case of digested DDP, the solubility was increased to 1.9 g/L as

Table 1
Solubility, water absorption, and hygroscopicity of whole and defatted date-pits.

Sample	Whole Date-Pits			Defatted Date-Pits		
	Solubility (g/L)	Water Absorption	Hygroscopicity	Solubility (g/L)	Water Absorption	Hygroscopicity
Untreated	1.3a	0.687a	0.111a	1.6a	0.748a	0.097a
Autoclaved	1.0b	0.672b	0.122b	1.2b	0.689b	0.109a
Digested	1.9c	0.673b	0.137c	1.9c	0.697b	0.191b

Note.
Expanded uncertainty, u(solubility): 0.06 g/L, u(water absorption): 0.005, u(hygroscopicity): 0.01.
Same letter in a column shows no significant differences ($P > 0.05$).

compared to autoclaved treatment ($P < 0.05$). This indicated that macromolecules of date-pits were damaged by the applied treatments.

The water absorption of untreated whole date-pits was 0.687 g water/g dry-solids, while this value was decreased to 0.672 g water/g dry-solids in case of autoclaved sample ($P < 0.05$). Sayas-Barbera et al. [42] reported that date-pits powder showed water absorption of 1.6 g of water/g sample. Cadavid et al. [34] observed water absorption of asparagus fiber ranged from 9.9 to 14.3 g/g fiber. Similarly, water absorption of peach pulp fiber and lemon fibers were 12.6 g/g fiber [43] and 11 g/g fiber [44], respectively. This indicated water absorption of date-pits was observed much lower than other types of pulp. The water absorption of digested WDP (i.e. 0.673 g water/g dry-solids) did not show any significant change as compared to the autoclaved sample ($P > 0.05$). The hygroscopicity values of untreated and autoclaved WDP were 0.111 and 0.122 g water/g sample, respectively. In the case of digested WDP, hygroscopicity value was increased as compared to the autoclaved sample ($P < 0.05$). This indicated mold digestion transformed the date-pits to more hydrophilic (i.e. created higher polar sites).

3.4. Proton mobility of whole date-pits

Fig. 3A shows a plot of ln ($S_2/S_{2,0}$) *versus* time for untreated whole date-pits within the whole relaxation time. Three linear segments indicated the existence of three types of protons in the whole date-pits. The relaxation times and intensities of rigid protons (T_{2b}), semi-rigid protons (T_{21}) and mobile protons (T_{22}) for untreated whole date-pits were identified from the slopes and intercepts (Fig. 3B, C and 3D). Similarly, Al-Mawali et al. [27] observed three linear segments in the case of whole date-pits. Values of T_{2b}, T_{21} and T_{22} of date-pits were considered as the rigid, semi-rigid and mobile protons mobility, respectively. Similarly, Srikaeo et al. [45] observed three linear segments (T_{2b}, T_{21} and T_{22}) in the waxy and non-waxy rice. The T_{2b} was assigned to rigid protons in macromolecule, T_{21} was assigned to semi-rigid protons in the monolayer-adsorbed water and T_{22} was assigned to mobile protons in the multilayer adsorbed water. In the case of dry soya beans, Li et al. [46] identified four segments of protons (i.e. T_{2b} was assigned for the protons of macromolecule, T_{21} and T_{22} for the protons in the strongly and weakly bound water molecules and T_{23} for the pools of protons in oil).

The relaxation times (i.e. T_{2b}, T_{21} and T_{22}) of untreated, autoclaved, digested WDP are presented in Table 2. Untreated whole date-pits showed T_{2b} and T_{22} as 14.36 μs and 56.9 ms, respectively, while these values decreased to 14.07 μs and 50.1 ms in the case of autoclaved treatment ($P < 0.05$). However, there was significant change in T_{21} between untreated and autoclaved treatments ($P < 0.05$). In the case of digested WDP, relaxation times of rigid (i.e. T_{2b}) and mobile (i.e. T_{22}) protons decreased as compared to autoclaved samples ($P < 0.05$). However, no significant difference was observed in T_{21} between digested and autoclaved samples. The higher relaxation time indicated lower mobility (i.e. stiff) of the protons [28]. Thus, the decrease of T_{2b}, and T_{22} in digested WDP samples indicated that digestion increased the mobility of these protons. This indicated that the structural damage as well as interference of the neighboring protons reduced their mobility.

3.5. Proton mobility of defatted date-pits

The relaxation times T_{2b}, T_{21} and T_{22} of DDP samples are presented in Table 2. The untreated DDP showed T_{21} and T_{22} as 0.52 ms and 78.9 ms, respectively, while these values increased in the case of autoclave treatment ($P < 0.05$). In the case of the digested DDP, T_{21} (i.e. 0.90 ms) and T_{22} (i.e. 68.1 ms) decreased ($P < 0.05$) as compared to autoclaved treatment, whereas T_{2b} (i.e. 11.39 μs) did not

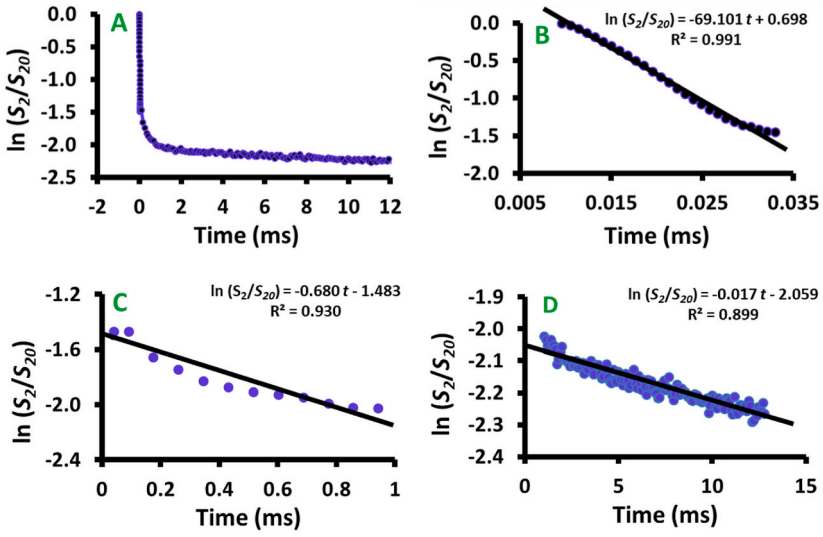

Fig. 3. Typical LF-NMR signal intensity of whole date-pits as a function of relaxation time, A: ln($S_2/S_{2,0}$) versus relaxation time, B: First linear part (i.e. rigid proton pools), C: Second linear part (i.e. rigid proton pools), D: Third linear part (i.e. rigid proton pools).

Table 2
Relaxation times of whole and defatted date-pits treatments as measured by LF-NMR.

Sample	Whole Date-Pits			Defatted Date-Pits		
	T_{2b} (μs)	T_{21} (ms)	T_{22} (ms)	T_{2b} (μs)	T_{21} (ms)	T_{22} (ms)
Untreated	14.36a	1.28a	56.9a	10.02a	0.52a	78.9a
Autoclaved	14.07b	1.46b	50.1b	11.23b	2.50b	70.9b
Digested	12.28c	1.33b	43.5c	11.39b	0.90c	68.1c

Note.
Expanded uncertainty, u(T_{2b}): 0.07 μs, u(T_{21}): 0.06 ms, u(T_{22}): 1.9 ms
Same letter in a column shows no significant differences (P > 0.05).

show any significant change (P > 0.05). This indicated that digestion enhanced mobility of the semi-rigid and mobile protons present in the macromolecules.

3.6. Thermal characteristics of treated whole date-pits

Fig. 4A shows the heat flow curve of the untreated WDP. This shows a structural relaxation with a change in slope or inflection point (i.e. marked as S) followed by a shift in the heat flow (i.e. glass transition marked as G) (Fig. 4A). An exothermic increase was observed due to cold crystallization or molecular ordering (i.e. marked as E) after solids melting-decomposition endothermic peak (i.e. marked as M) (Fig. 4A). A minor endothermic peak was observed due to the melting of oil at the structural relaxation S (Fig. 4B). This structural relaxation could be due to the melting of oil. A clear structural relaxation at the glass transition can be visualized in Fig. 4C. The structural relaxation was observed at −3.2 °C, and the onset glass transition was observed at 138 °C with a specific heat change (295 J/kg °C) at the glass transition (Table 3). Al-Mawali et al. [27] observed the oil-melting peak at 2.8 °C, which was close to the structural relaxation. Similarly, they observed the onset of glass transition temperature of air-dried whole date-pits at 138 °C. In the case of freeze-dried date-pits, Suresh et al. [47] observed lower glass transition within 43–50 °C. However, Rahman et al. [25] were unable to observe a shift in the case of roasted date-pits and they explained that this could be due to the complexity of glass transition in the case of very compact rigid biomaterial. The complexity and multi-factors of the glass transition could be beyond the simplicity of the thermal analysis as measured by DSC. In the case of roasted coffee beans, Rivera et al. [48] were unable to observe a shift in the heat flow. Rather they observed an inflection in the heat flow curve. They pointed out that roasting transformed more compact ordered molecules in the coffee beans, which caused low specific heat change at the glass transition. Date-Pits possessed different rigidity due to their complex multi-domain interactions of the amorphous and crystalline domains. This could cause the difference or absence of the

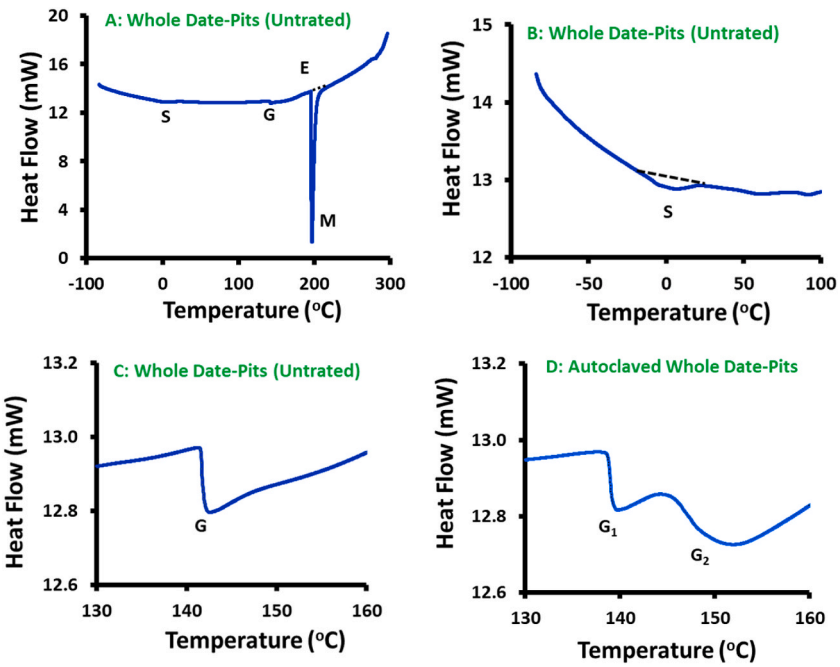

Fig. 4. DSC thermogram of WDP, autoclaved WDP and Digested WDP, A: WDP (−90 to 300 °C), B: WDP (−90 to 100 °C), C: WDP (130–160 °C), D: Autoclaved WDP (−90 to 300 °C), E: Autoclaved WDP (−90 to 100 °C), F: WDP (130–160 °C), G: Digested WDP (−90 to 200 °C), H: Digested WDP (−90 to 100 °C), I: Digested WDP (130–160 °C).

Table 3
Glass transition of treated (autoclave and mold digestion) and untreated whole date-pits.

Sample	First Glass Transition					Second Glass Transition				
	T_s (°C)	T_{gi} (°C)	T_{gp} (°C)	T_{ge} (°C)	$(\Delta C_p)_1$ (J/kg °C)	T_{gi} (°C)	T_{gp} (°C)	T_{ge} (°C)	$(\Delta C_p)_2$ (J/kg °C)	$(\Delta C_p)_T$ (J/kg °C)
Untreated	−3.2a	138a	138a	139a	295a	N	N	N	N	295
Autoclaved	−0.5b	137a	137a	138a	197b	145a	146a	147a	170a	367
Digested	−7.1c	138a	138a	139a	155c	147b	148b	149a	173a	328

Note.
Expanded uncertainty, u(T_s): 1.0 °C, u(T_{gi}): 0.7 °C, u(T_{gp}): 0.7 °C, u(T_{ge}): 0.7 °C, u[$(\Delta C_p)_1$]: 10 J/kg °C, u[$(\Delta C_p)_2$]: 10 J/kg °C.
Same letter in a column shows no significant differences ($P > 0.05$).

glass transition in the date-pits biomaterial containing a complex structure [47].

In the case of autoclaved whole date-pits, structural relaxation, glass transition, exothermic increase and solids melting-decomposition were observed. In this case, two shifts (i.e. two glass transitions marked as G_1 and G_2) were observed before the exothermic increase (Fig. 4D). In the literature, multiple glass transitions were detected in the cases of dried papaya [49], dried rice [50] and freeze-dried tuna meat [51]. The existence of the multiple glass transition was due to the molecular incompatibility, natural heterogeneity and phase separation of different rubbery domains in the complex biomaterials [52,53]. The relaxation temperature of autoclaved WDP shifted to a higher temperature at −0.5 °C ($P < 0.05$), while there was no significant change to the onset glass transition temperature ($P > 0.05$) (Table 4). However, a specific heat change at the glass transition temperature decreased to 197 J/kg °C (Table 4). This decrease in the specific heat change at the glass transition indicated that autoclave caused the formation of more ordered molecules. In the case of digested samples, similar characteristics to WDP, and autoclaved WDP were observed in the heat flow curves. The structural relaxation temperatures of digested WDP decreased to lower values as compared to the autoclaved whole date-pits ($P < 0.05$), while minor changes were observed in the case of first glass transition temperature (Table 3). However, specific heat at the first glass transition decreased in the case of digested WDP.

The second glass transition in the cases of untreated, autoclaved and digested WDP, and their specific heat change are presented in Table 3. The untreated WDP did not show the second glass transition, while autoclaved and digested WDP showed the second glass transition. The digested WDP showed an insignificant difference in the specific heat change at the second glass transition ($P < 0.05$). The total specific heat changes for untreated, autoclaved, and digested WDP were observed as 295, 367 and 328 J/kg °C, respectively. The lower specific heat change indicated that more ordered phases were formed because of the digestion by molds. This indicated that mold was acting on the amorphous part of the whole date-pits. Sperandio et al. [54] reported that *T. reesei* and its mutant strains produced cellulase (i.e.enzyme) and these are heavily used as a source of carbohydrate-active enzymes. They hydrolyze lignocellulose substrates into fermentable sugars. Similarly, Alyileili et al. [55] observed that *T. reesei* secreted enzymes to catalyze the degeneration of lignocellulosic substrates in date-pits and then formed simple sugars, thus enhanced the degradation of plant cell walls.

Thermal characteristics (i.e. solids melting-decomposition) of untreated, autoclaved, and digested WDP are presented in Table 4. The onset solids melting-decomposition temperature of untreated whole date-pits was observed at 194 °C with a peak at 196 °C. The onset solids melting-decomposition temperatures did not change by autoclaved treatment ($P > 0.05$). Similarly, there were no significant differences between the onset and mid-solids melting-decomposition temperatures between autoclaved and digested WDP ($P > 0.05$). The end of solids melting-decomposition temperature in the autoclaved sample decreased significantly as compared to the untreated sample. However, the end of solids melting-decomposition point of digested sample increased significantly in comparison with the autoclaved sample. The onset and peak solids melting-decomposition temperatures of WDP was observed at 179 °C and ended at 200 °C, which was lower as compared to the values as observed in the current study [27]. Suresh et al. [47] observed the onset, peak and end solids-melting temperatures of freeze-dried date-pits at 59, 106 and 197 °C, respectively. These temperatures were much lower as compared to the WDP a prepared by air-dried in this study.

The enthalpy of the endothermic peak was observed as 68 J/g in the case of untreated sample and it increased significantly to 78 J/g in the case of the autoclaved sample. The enthalpy of solids melting-decomposition was observed as 125 J/g in whole date-pits, which was higher than enthalpy as observed in this study [27]. This higher enthalpy was due to the high moisture content as compared to this study. Suresh et al. [47] observed the enthalpy of freeze-dried date-pits was 184 J/g, which was much higher as compared to the whole date pits used in this study. This could be due to higher moisture content and different drying methods (i.e.

Table 4
Solids melting-decomposition of whole and defatted date-pits as measured by DSC.

Sample	Whole Date-Pits				Defatted Date-Pits			
	T_{mi} (°C)	T_{mp} (°C)	T_{me} (°C)	ΔH (J/g)	T_{mi} (°C)	T_{mp} (°C)	T_{me} (°C)	ΔH (J/g)
Untreated	194a	196a	209a	68a	213a	214a	224a	60a
Autoclaved	191a	193a	203b	78b	194b	195b	209b	81b
Digested	196a	198a	208a	62c	200b	201b	212b	87b

Note.
Expanded uncertainty, u(T_{mi}): 1.5 °C, u(T_{mp}): 1.1 °C, u(T_{me}): 0.9 °C, u(ΔH): 1.7 J/g.
Same letter in a column shows no significant differences ($P > 0.05$).

freeze-drying and air-drying) used as compared to this study. This also indicated the existence of stronger molecular bonding in freeze-dried date-pits as compared with air-dried whole date-pits. The enthalpy showed significant differences between autoclaved sample and treated sample (i.e. 62 J/g). The digested WDP showed the lowest enthalpy indicating the formation of weaker internal bonds due to digestion by molds, thus lower energy was required to decompose the solids.

3.7. Thermal characteristics of treated defatted date-pits

Fig. 5 shows the heat flow curves for the untreated, autoclaved and digested DDP. It shows two shifts in the heat flow (i.e. two glass transitions marked as G_1 and G_2) followed by an exothermic increase that was observed due to cold crystallization or molecular ordering (i.e. marked as E) and solids melting-decomposition endothermic peak (i.e. marked as M) (Fig. 5A, B and 5C). In the case of DDP, the structural change did not observe. Clear glass transitions can be visualized in Fig. 5C. The onset of the first glass transition was observed at 159 °C with a specific heat change 473 J/kg ^{o}C (Table 5). All defatted date-pits samples did not show structural relaxation and oil-melting peak (Fig. 5B). In the cases of autoclaved and digested defatted date-pits, endothermic peaks were observed after the second glass transition (Fig. 5D). Therefore, there was a relaxation process after the second glass transition. Rahman et al. [25] did not observe glass transition in roasted-defatted date-pits powder. The onset first glass transition temperature of autoclaved defatted date-pits shifted to a lower temperature at 135 °C with a specific heat change to 279 J/kg ^{o}C ($P < 0.05$). However, onset first glass transition temperature and the specific heat change of digested DDP increased significantly as compared to the autoclaved defatted date-pits ($P < 0.05$) (Table 5).

The second glass transition of untreated, autoclaved, and digested DDP and their specific heat change are presented in Table 5. The onset of the glass transition temperature of the second shift of untreated DDP was observed at 164 °C with a specific heat change to 305 J/kg ^{o}C. In the case of autoclaved treatment, the onset glass transition shifted to a lower temperature at 146 °C, while the specific change increased to 1050 J/kg ^{o}C ($P < 0.05$). However, there was no significant difference for the onset of the second glass transition temperature of the digested sample ($P > 0.05$), while the specific heat change increased to 1573 J/kg ^{o}C as compared to autoclave treatment ($P < 0.05$). The specific heat changes for untreated, autoclaved, digested DDP were observed as 778, 1329, and 1877 J/kg ^{o}C, respectively (Table 5). The higher specific heat indicated a more amorphous phase was formed because of the digestion by molds, indicating mold is working on the crystalline part of the DDP.

Solids melting-decomposition of untreated, autoclaved, and digested DDP are presented in Table 4. The onset solids melting-decomposition temperature of untreated defatted date-pits was observed at 213 °C with a peak at 214 °C. The enthalpy of the peak was 60 J/g. Orozco et al. [56] observed the peaks at around 240 °C could be due to the onset of the solids melting-decomposition of hemicellulose in fruit wastes (orange bagasse and orange, banana, and mango peels) which were higher as compared to values observed in the case of DDP. In the case of autoclaved treatment, the solids melting-decomposition temperatures decreased

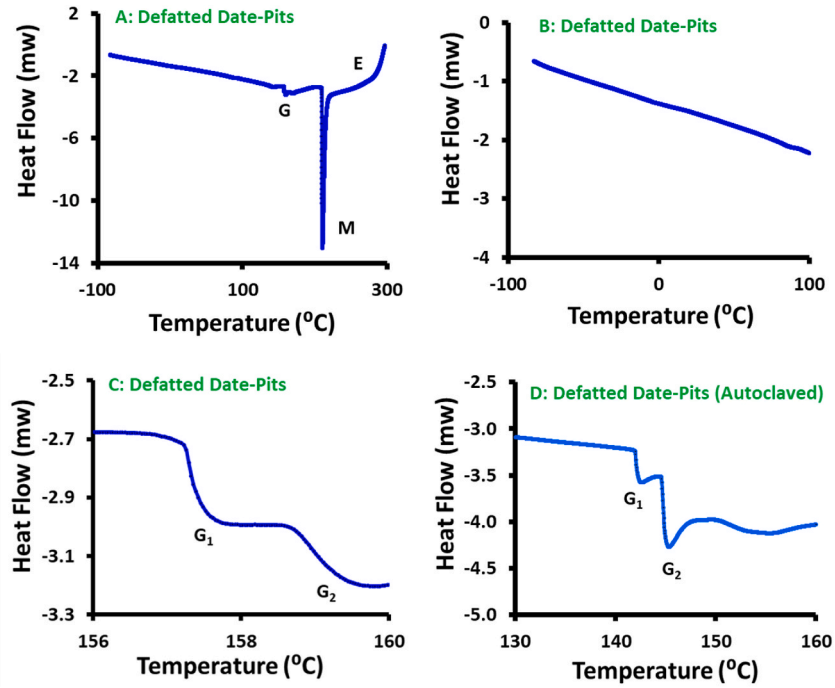

Fig. 5. DSC thermogram of DDP, autoclaved DDP and Digested DDP, A: DDP (−90 to 300 °C), B: DDP (−90 to 100 °C), C: DDP (156–160 °C), D: Autoclaved DDP (−90 to 300 °C), E: Autoclaved DDP (−90 to 100 °C), F: DDP (130–160 °C), G: Digested DDP (−90 to 200 °C), H: Digested DDP (−90 to 100 °C), I: Digested DDP (130–160 °C).

Table 5
Glass transition of treated (autoclave and mold digestion) and untreated defatted date-pits.

Sample	First Glass Transition				Second Glass Transition				
	T_{gi} (°C)	T_{gp} (°C)	T_{ge} (°C)	$(\Delta C_p)_1$ (J/kg °C)	T_{gi} (°C)	T_{gp} (°C)	T_{ge} (°C)	$(\Delta C_p)_2$ (J/kg °C)	$(\Delta C_p)_T$ (J/kg °C)
Untreated	159a	160a	161a	473a	164a	164a	165a	305a	778a
Autoclaved	135b	135b	135b	279b	146b	147b	148b	1050b	1329b
Digested	138c	138c	138c	304c	148b	149b	150b	1573c	1877c

Note.
Expanded uncertainty, u(T_{gi}): 2.1 °C, u(T_{gp}): 2.2 °C, u(T_{ge}): 2.4 °C, u[$(\Delta C_p)_1$]: 3 J/kg °C, u[$(\Delta C_p)_2$]: 8 J/kg °C.
Same letter in a column shows no significant differences ($P > 0.05$).

significantly, while the enthalpy increased to 81 J/g ($P < 0.05$). The solid melting temperatures and enthalpy of the digested DDP (87 J/g) showed no significant change as compared to the autoclaved sample. The DNR sample showed the highest enthalpy indicating that it contained stronger internal bonds, thus more energy was needed to decompose the solid matrix with high water content.

3.8. Functional-groups characteristics of treated WDP

Fig. 6 shows the FTIR spectroscopy of untreated, autoclaved and digested WDP and DDP. The autoclaved spectra showed higher absorption for all selected functional groups as compared to the untreated WDP (Fig. 6A). The higher absorption at each peak indicates the damage to the bonds in their functional groups. The spectrum of untreated whole date-pits powder showed a wider peak of 2800–3700 cm^{-1} due to the OH group stretching. Sohail et al. [57] identified a peak of O–H stretching at 3400 cm^{-1} in the case of air-dried raw date-pits powder, and Sharfan et al. [58] observed a wider peak for whole date-pits in the range of 3200–3400. Similarly, Nabili et al. [36] observed a wider peak of date-pits powder at 3367 cm^{-1} assigned to O–H group stretching vibrations in hydroxyl groups. The sharp peaks at this location showed the existence of inter and intra interactions of OH groups in the cellulose structure [59]. The shift of this peak to a higher intensity and existence of a narrower peak indicated the splitting of hydrogen bonds [59]. In the case whole date-pits, OH peak showed relatively lower intensity as compared to the date-pits powder [58]. This could be due to the intake structure of the date-pits as compared to the damaged structure in the case of date-pits powder.

The characteristic bands at 3000-2800 cm^{-1} were attributed to C–H stretching of methyl and methylene groups. Nabili et al. [36]

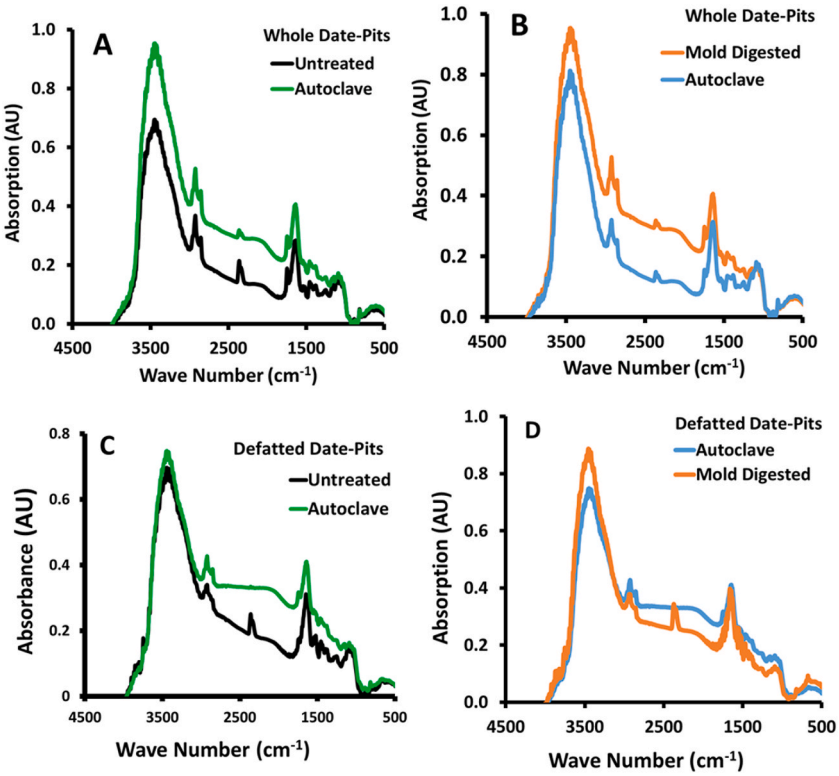

Fig. 6. FTIR spectra, A: WDP (untreated and autoclaved), B: WDP (autoclaved and mold digested), C: DDP (untreated and autoclaved), D: DDP (autoclaved and mold digested).

observed a peak at 2924 cm^{-1}, which corresponded to asymmetric C–H bands in methyl and methylene groups. Commonly, cellulose, hemicellulose and lignin contribute to these characteristic bands [60]. The peak at 2855 cm^{-1} was attributed to symmetric C–H bands in methyl and methylene groups, assigned to cutin and waxes. The peak at 2910 cm^{-1} was assigned to the carbohydrate methyl C–H stretching from lignocellulose fibers [61]. Byrne et al. [62] proposed that this could be due to antisymmetric expansion and contraction of C–H. Similarly, Sharfan et al. [58] observed similar peaks of C–H and CH_2 or CH_3 bands within the 2800-2900 cm^{-1}.

In the range of 1600–1800 cm^{-1}, two peaks were identified which could correspond to carbonyl C═O and alkenyl C═C stretching. The C═O stretch vibrations assigned to aldehydes and generally identified in the range of 1735 cm^{-1} [63,64]. Sohail et al. [57] observed a peak at 1744 cm^{-1} assigned to C═O stretching. Sharfan et al. [58] observed this peak at 1740 cm^{-1} band for the WDP. This was due to the existence of unsaturated organic compounds, for examples aldehydes, ketones, and ester groups present in the hemicellulose [58]. Nabili et al. [36] determined a peak at 1744 cm^{-1} corresponding to carbonyl C═O stretching. They pointed that this could be due to following functional groups: (i) the acetyl, and uronic ester groups of hemicelluloses, (ii) ester linkage of carboxylic groups of the ferulic and (iii) *p*-coumaric acids of lignin and/or hemicelluloses. They also observed a band at 1616 cm^{-1} which could be attributed to C═C or C═N vibrations in the aromatic region. Sun et al. [61,65] identified a peak at 1639 cm^{-1} assigned to the bending mode of the adsorbed water to the solid matrix. However, Sharfan et al. [58] pointed out 1629 cm^{-1} could be related to C–O stretching of carboxyl or carbonyl group.

Several vibrations were observed in the range of 1500-1000 cm^{-1}. Nabili et al. [36] identified the bands at 1522 and 1437 cm^{-1} due to C═C stretch of the aromatic skeletal mode, while Sharfan et al. [58] observed these at 1526 and 1458 cm^{-1} bands. Nabili et al. [36] also determined a peak at 1377 cm^{-1} corresponded to C–H stretch of cellulose and a peak at 1246 cm^{-1} due to C–O–H deformation and C–O stretch of phenolic compounds. The peak at 1061 cm^{-1} represented the C–O stretch vibration of hemicellulose and cellulose. In

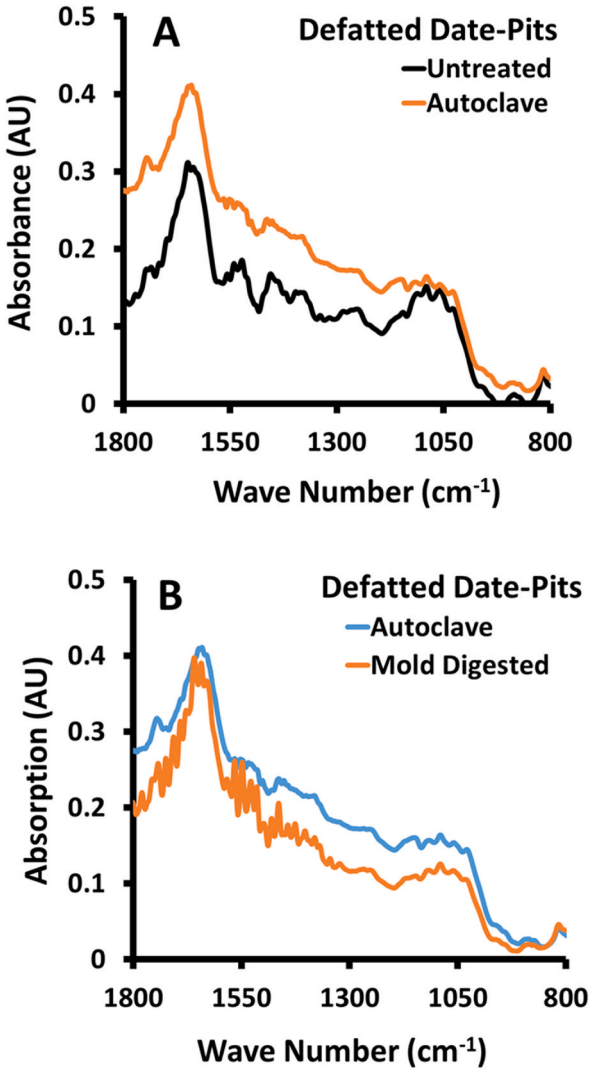

Fig. 7. FTIR spectra of DDP within wave number 1800 and 800 cm^{-1}, A: untreated and autoclaved, B: autoclaved and mold digested.

the case of whole date-pits, Sharfan et al. [58] observed a strong peak at 1012 cm^{-1} band due to the bending vibration of organic compounds of C–O bond. Sohail et al. [57] observed different forms of vibration in the range of 1300-1000 cm^{-1} due to C═O, C–H, C–O stretches and a peak at 1158 cm^{-1} assigned to C–*O*–C stretching. A peak at 1428 cm^{-1} was assigned due to the CH_2 bending and 1374 cm^{-1} band was assigned to the O–H bending [61]. In addition, the band at 1328 cm^{-1} was produced by the C–C and C–O skeletal vibrations [66]. The peak observed at 1169 cm^{-1} attributed to C–O antisymmetric bridge stretching and the band at 1076-1023 cm^{-1} due to C–O–C pyranose ring skeletal vibration [61,67]. The absorption peaks at 900-800 cm^{-1} could be due to the C–H rocking vibrations of cellulose, and Nabili et al. [36] observed a peak at 870 cm^{-1}. The peaks at 872 and 808 cm^{-1} bands was assigned to aldehyde and derivatives of benzenes group [58]. Similar absorption peaks with higher intensities were observed in the spectra of the autoclaved and digested WDP (Fig. 6B). This indicated that bonds in the functional group became more-damaged in the digested sample.

3.9. Functional-groups characteristics of treated DDP

The spectra of untreated and autoclaved DDP showed a wider peak within 2800–3700 cm^{-1} due to the OH group stretching (Fig. 6C). The untreated date-pits spectrum showed lower absorption at this peak as compared to the autoclaved sample. Adewole et al. [68] observed the broad band at 3417 cm^{-1} due to hydrogen bonding in the case of defatted date-pits. Al-Khalili et al. [35] identified a wider peak at 3325 cm^{-1} in defatted date-pits. Sun et al. [61] attributed the peak at 3420 cm^{-1} to O–H stretching and C–H group stretching. All spectra showed two peaks at 3000-2800 cm^{-1} with higher intensities in the case of autoclaved treatment. These were attributed to C–H stretching of methyl and methylene groups. Similarly, Al-Khalili et al. [35] identified two sharp peaks at 2925 and 2850 cm^{-1}. Adewole et al. [68] identified a band at 2925 cm^{-1}, which was assigned to methylene (C–H) stretching vibration.

In the range of 2300–2500 cm^{-1}, the untreated spectrum showed a peak, while this peak was absent in the case of the autoclaved sample spectrum. In the range of 1600–1800 cm^{-1}, two peaks were identified corresponding to carbonyl C═O and alkenyl C═C stretching. Al-Khalili et al. [35] observed a peak at 1740 cm^{-1}, which was attributed to acetyl groups in the sample. They identified an adsorbed water band within 1640–1660 cm^{-1}. Adewole et al. [68] determined a band at 1630 cm^{-1} due to the presence of carbonyl compound. Several bands in the range of 1500-1000 cm^{-1} were identified. Adewole et al. [68] determined peaks at 1520, 1442, and 1381 cm^{-1} that were due to aromatics compounds and a band at 1060 cm^{-1} that was assigned to CH–O–CH stretching. Al-Khalili et al. [35] observed peaks in the case of defatted date-pits at 1381 and 1450 cm^{-1}. Saccharides can be characterized by the variable-angle vibration bands at 1436 and 1440 cm^{-1} [69]. The absorption at 1261 cm^{-1} could be due to OH in-plane bending cellulose [61]. In the case of the digested DDP, the spectrum showed higher absorption for the hydroxyl group as compared to autoclave treatment (Fig. 6D). This indicated that mold digestion caused more damage to the hydroxyl group. The damage of the date-pits fibers was also evident from the thermal and NMR analysis. However, it was evident a lower absorption for the other functional groups as compared to autoclaved sample. This indicated that bonds present in the functional group became stiffer due to the digestion by the mold. In addition, in the case of digested DDP, as compared to the autoclaved (Fig. 7A), digested one (Fig. 7B) showed many absorption peaks (i.e. splitting the peaks) within the band of 1800-1400 cm^{-1} (Fig. 7). This indicated that functional groups within this range were damaged or affected by surrounding functional groups.

3.10. Applications of digested date-pits

Dietary fibers in date-pits can have several physicochemical properties including solubility, water absorption, fermentability, viscosity and binding ability when applied to foods [70]. These dietary fibers show different types of health benefits [71] and can be categorized into two groups, soluble and insoluble, based on their water solubility. The soluble dietary fiber includes pectin, inulin and gums, whereas the insoluble dietary fiber includes cellulose, hemicelluloses and lignin [70]. The preparation of functional digested date-pits fibers could be applied to different food products, such as dairy, bread, baked products, noodles, pasta and soups. It could provide more functionality as compared to the untreated date-pits powder. This could be due to the high hydrophilic characteristics, highly amorphous, and damaged structure of the mold digested date-pits. Soluble or amorphous fibers can form a gel-like structure in the gastrointestinal track and play a role in lowering cholesterol and glucose levels [72]. Douglas [73] explained that gels and viscous mass are amorphous solids and these can form cross-linking and physical associations with entangled interactions. Consequently, these interactions can lead to gel-like structures or amorphous solidification.

More interactions in the food matrix could be achieved by damaged fibers. Horie et al. [74] explained that the damage of macromolecular compounds by dissociation or detachment ultimately produced fragments with reactive end-groups and could form crosslinks having different molecular structure [75]. The amorphous fraction can be considered as soluble fibers [76] and this can create sol-gel like structure [77]. It was also expected that more availability of free health functional and antibacterial bioactive compounds, such as polyphenols, and flavones [23,78]. Munoz-Tebar et al. [1] highlighted the potential of date-pits flour for the food industry due to its fiber content, essential fatty acids, and bioactive compounds. This could generate value added bio-products by reducing the amount of generated waste from food industry and thus promoting the circular economy in the foods and biomaterials chain. Pretreatments are necessary if lignocellulose materials, such as date-pits are used as an ingredient for the fermentation process, for example lactic acid production. The effective hydrolysis could be hindered due to the structure of lignocellulose when the access of enzymes to cellulose and hemicellulose fibers is restricted in the solids matrix [79]. In the case of alkaline treatment, formic acid, acetic acid, and coumaric acid were found inhibitory effect on the fermentation of lactic acid, and furfural was the major inhibitory compound in the case of acid pretreat [79]. The absent of these inhibitory compounds in mold treated date-pits could be beneficial and safe when these are used as ingredients in the fermentation process.

4. Conclusion

In the present study, whole and defatted date-pits were digested by *T. reesei* at high moisture content. Four phases (i.e. lag, exponential, stationary, and death) were observed for the growth of *T. reesei* in the digested WDP and DDP. However, DDP digestion showed higher mold growth as compared to the WDP, indicating that *T. reesei* used date-pits as nutrients for their growth and proliferation. The high solubility and hygroscopicity of the digested WDP and DDP by mold indicated macromolecules damage and increased hydrophilic fraction. Autoclaved WDP showed lower T_{2b} and T_{22} as compared to the untreated WDP ($P < 0.05$), while there was no significant change in the case of T_{21}. The untreated DDP showed lower T_{21} and T_{22} as compared to the autoclaved DDP ($P < 0.05$). This indicated that digestion transformed these protons to high mobility due to structural damage and interference of the neighboring protons. The heat flow of the untreated WDP showed a structural relaxation and glass transition followed by an exothermic increase due to cold crystallization or molecular ordering before the solids melting-decomposition endothermic peak. The mold digestion created a 5.7 times amorphous fraction in the DDP (ΔC_p: 1877 J/kg ^{o}C) as compared to the WDP (ΔC_p: 328 J/kg ^{o}C). The FTIR spectra showed different types of damage in the cases of WDP and DDP also evidenced by the degree of mold growth. Overall, mold digestion caused molecular structural damage with enhanced amorphous fraction, thus enhancing its ability to interlink with other components when applied to foods and other bio-composites.

CRediT authorship contribution statement

Samar Mohammed Khalaf Al-Saidi: Writing – original draft, Methodology, Investigation, Formal analysis, Data curation, Conceptualization. **Zahra Sulaiman Nasser Al-Kharousi:** Formal analysis, Data curation, Conceptualization. **Mohammad Shafiur Rahman:** Writing – review & editing, Writing – original draft, Resources, Project administration, Funding acquisition, Formal analysis, Data curation, Conceptualization. **Nallusamy Sivakumar:** Writing – review & editing, Data curation, Conceptualization. **Ansar Rasul Suleria:** Writing – review & editing, Formal analysis, Data curation, Conceptualization. **Muthupandian Ashokkumar:** Writing – review & editing, Formal analysis, Conceptualization. **Malik Hussain:** Writing – review & editing, Conceptualization. **Nasser Al-Habsi:** Writing – review & editing, Funding acquisition, Formal analysis, Data curation, Conceptualization.

Declaration of competing interest

The authors declare that they have no known competing financial interests or personal relationships that could have appeared to influence the work reported in this paper.

Acknowledgements

This research was funded by the His Majesty Trust Funds (SR/AGR/FOOD/2019/1). The major focus of this project was to develop value added functional bio-products from food waste and the valorization could bring gain to the economic gain and circular economy.

References

[1] N. Munoz-Tebar, L. Candela-Salvador, J.A. Perez-Alvarez, J.M. Lorenzo, J. Fernandez-Lopez, M. Viuda-Martos, Date (*Phoenix dactylifera* L. cv. Medjool) seed flour, a potential ingredient for the food industry: effect of particle size on its chemical, technological, and functional properties, Plants 13 (2024) 1–13 (Article 335.

[2] M.A. Al-Farsi, C.Y. Lee, Usage of date (Phoenix dactylifera L.) seeds in human health and animal feed, Nuts and Seeds in Health and Disease Prevention (2011) 447–452.

[3] M. Wahini, Exploration of making date seed's flour and its nutritional contents analysis. IOP Conference Series, Mater. Sci. Eng. 128 (1) (2016) 012031.

[4] S.R. Alyileili, K.A. El-Tarabily, I.E. Belal, W.H. Ibrahim, M. Sulaiman, A.S. Hussein, Effect of Trichoderma reesei degraded date pits on antioxidant enzyme activities and biochemical responses of broiler chickens, Front. Vet. Sci. 7 (2020), 31-10 (Article338).

[5] M.Z. Hossain, M.I. Waly, V. Singh, V. Sequeira, M.S. Rahman, Chemical composition of date-pits and its potential for developing value-added product-a review, Pol. J. Food Nutr. Sci. 64 (4) (2014) 215–226.

[6] M. Al-Bowait, S.I. Al-Sultan, The effect of partial replacement of maize by alkali-treated date pits on broiler growth, survival rate and economic returns, Livest. Res. Rural Dev. 19 (9) (2007). Article 121.

[7] W. Al-Shahib, R.J. Marshall, The fruit of the date palm: its possible use as the best food for the future, Int. J. Food Sci. Nutr. 54 (4) (2003) 247–259.

[8] H.A. Almana, R.M. Mahmoud, Palm date seeds as an alternative source of dietary fiber in Saudi Bread, Ecol. Food Nutr. 32 (1994) 261–270.

[9] O. Ishrud, M. Zahid, V.U. Ahmad, Y. Pan, Isolation and structure analysis of a glucomannan from the seeds of Libyan dates, J. Agric. Food Chem. 49 (8) (2001) 3772–3774.

[10] A.E. Bawazir, A.A. Saddiq, Antimicrobial activity of date palm (*Phoenix dactylifera*) pits extracts and its role in reducing the side effect of methyl prednisolone on some neurotransmitter content in the brain, hormone testosterone in adulthood, IV International Date Palm Conference 882 (2010) 665–690.

[11] S.A. Jassim, M.A. Naji, In vitro evaluation of the antiviral activity of an extract of date palm (*Phoenix dactylifera L.*) pits on a *Pseudomonas* phage, Evid. base Compl. Alternative Med. 7 (1) (2010) 57–62.

[12] M. Al-Farsi, C. Alasalvar, M. Al-Abid, K. Al-Shoaily, M. Al-Amry, F. Al-Rawahy, Compositional and functional characteristics of dates, syrups, and their by-products, Food Chem. 104 (3) (2007) 943–947.

[13] M.A. Al-Farsi, C.Y. Lee, Optimization of phenolics and dietary fibre extraction from date seeds, Food Chem. 108 (3) (2008) 977–985.

[14] S. Saryono, W. Warsinah, A. Isworo, F. Efendi, Anti-inflammatory effect of date seeds (*Phoenix dactylifera L*) on carrageenan-induced edema in rats, Trop. J. Pharmaceut. Res. 17 (12) (2018) 2455–2461.

[15] A. Isworo, Anti-inflammatory activity of date palm seed by down regulating interleukin-1β, TGF-β, cyclooxygenase-1 and-2: a study among middle age women, Saudi Pharmaceut. J. 28 (8) (2020) 1014–1018.

[16] L. Ravi, Bioactivity of *Phoenix dactylifera* seed and its phytochemical analysis, Int. J. Green Pharm. 11 (2) (2017) S292–S297.

[17] M. Hasan, A. Mohieldein, In vivo evaluation of antidiabetic, hypolipidemic, antioxidative activities of Saudi date seed extract on streptozotocin induced diabetic rats, J. Clin. Diagn. Res. 10 (3) (2016) FF06–FF12.

[18] M.A. Al-Ghouti, J. Li, Y. Salamh, N. Al-Laqtah, G. Walker, M.N. Ahmad, Adsorption mechanisms of removing heavy metals and dyes from aqueous solution using date pits solid adsorbent, J. Hazard Mater. 176 (1–3) (2010) 510–520.
[19] E. Guiavarch, A. Pons, G. Christophe, C. Creuly, C.G. Dussap, Analysis of a continuous culture of *Fibrobacter succinogenes S85* on a standardized glucose medium, Bioproc. Biosyst. Eng. 33 (4) (2010) 417–425.
[20] H. Yu, G. Zeng, H. Huang, X. Xi, R. Wang, D. Huang, J. Li, Microbial community succession and lignocellulose degradation during agricultural waste composting, Biodegradation 18 (6) (2007) 793–802.
[21] D.E. Koeck, A. Pechtl, V.V. Zverlov, W.H. Schwarz, Genomics of cellulolytic bacteria, Curr. Opin. Biotechnol. 29 (2014) 171–183.
[22] A.V. Gusakov, Alternatives to *Trichoderma reesei* in biofuel production, Trends Biotechnol. 29 (9) (2011) 419–425.
[23] S.R. Alyileili, I.E.H. Belal, A.S. Hussein, K.A. El-Tarabily, Effect of inclusion of degraded and non-degraded date pits in broilers' diet on their intestinal microbiota and growth performance, Animals 10 (2020) 1–13 (Article 2041).
[24] Y. Roos, M. Karel, Applying state diagrams to food processing and development, Food Technol. 45 (12) (1991) 66–68.
[25] M.S. Rahman, S. Kasapis, N.S.Z. Al-Kharusi, I.M. Al-Marhubi, A.J. Khan, Composition characterisation and thermal transition of date pits powders, J. Food Eng. 80 (1) (2007) 1–10.
[26] P. Gill, T.T. Moghadam, B. Ranjbar, Differential scanning calorimetry techniques: applications in biology and nanoscience, J. Biomol. Tech. 21 (4) (2010) 167–193.
[27] M. Al-Mawali, N. Al-Habsi, M.S. Rahman, Thermal characteristics and proton mobility of date-pits and their alkaline treated fibers, Food Eng. Rev. 13 (1) (2020) 236–246.
[28] N.A. Al-Habsi, S. Al-Hadhrami, H. Al-Kasbi, M.S. Rahman, Molecular mobility of fish flesh measured by low-field nuclear magnetic resonance (LF-NMR) relaxation: effects of freeze–thaw cycles, Fisheries Science 83 (5) (2017) 845–851.
[29] U. Erikson, I.B. Standal, I.G. Aursand, E. Veliyulin, M. Aursand, Use of NMR in fish processing optimization: a review of recent progress, Magn. Reson. Chem. 50 (7) (2012) 471–480.
[30] G.S. Al-Saidi, A. Al-Alawi, M.S. Rahman, N. Guizani, Fourier transform infrared (FTIR) spectroscopic study of extracted gelatin from shaari (*Lithrinus microdon*) skin: effects of extraction conditions, Int. Food Res. J. 19 (3) (2012) 1167–1173.
[31] P. Chaiwut, P. Chomnunti, N. Thaochan, A. Saikeur, P. Pintathong, Effect of solid state fermentation with *Trichoderma spp*. on phenolic content and antioxidant capacities of mature Assam tea leaves, Journal of Food Science and Agricultural Technology 5 (2019) 106–113.
[32] S.A. Hassan, A.D. Altalhi, Y.A. Gherbawy, B.A. El-Deeb, Bacterial load of fresh vegetables and their resistance to the currently used antibiotics in Saudi Arabia, Foodborne Pathogens and Disease 8 (9) (2011) 1011–1018.
[33] AOAC, Official Methods of Analysis, fourteenth ed., Association of Official Analytical Chemists, Washington DC, 1995.
[34] A. Cadavid, E.L. Restrepo Molina, C.J.R. Valenzuela, Chemical, physicochemical and functional characteristics of dietary fiber obtained from asparagus byproducts (*Asparagus officinalis L.*), Rev. Fac. Nac. Agron. Medellín 68 (1) (2015) 7533–7544.
[35] M. Al-Khalili, N. Al-Habsi, A. Al-Alawi, L. Al-Subhi, M.T.Z. Myint, M. Al-Abri, M.S. Rahman, Structural characteristics of alkaline treated fibers from date-pits: Residual and precipitated fibers at different pH, Bioactive Carbohydrates and Dietary Fibre 25 (2021) 1–11 (Article 100251).
[36] A. Nabili, A. Fattoum, R. Passas, E. Elaloui, Extraction and characterization of cellulose from date palm seeds (*Phoenix dactylifera L.*), Cellul. Chem. Technol. 50 (2016) 1015–1023.
[37] MS-Excel, Statistical Software, 2010. Microsoft, US.
[38] C. Altieri, D. Cardillo, A. Bevilacqua, M. Sinigaglia, Inhibition of *Aspergillus spp*. and *Penicillium spp*. by fatty acids and their monoglycerides, J. Food Protect. 70 (5) (2007) 1206–1212.
[39] J. Krisch, R. Tserennadmid, C. Vágvölgyi, Essential oils against yeasts and moulds causing food spoilage, in: Science against Microbial Pathogens: Communicating Current Research and Technological Advances,, 2011, pp. 1135–1142. Badajoz, Spain.
[40] R. Bressani, J.C. Turcios, L. Reyes, R. Mérida, Physical and chemical characterization of nixtamalized industrial corn flours for human consumption in Central America, Latin American Archives of Nutrition 51 (3) (2001) 309–313.
[41] C.M. Rosell, E. Santos, C. Collar, Physico-chemical properties of commercial fibres from different sources: a comparative approach, Food Res. Int. 42 (1) (2009) 176–184.
[42] E. Sayas-Barberá, A.M. Martín-Sánchez, S. Cherif, J. Ben-Abda, J.Á. Pérez-Álvarez, Effect of date (*Phoenix dactylifera L.*) pits on the shelf life of beef burgers, Foods 9 (1) (2020) 1–15 (Article 102).
[43] N. Grigelmo-Miguel, O. Martín-Belloso, Comparison of dietary fibre from by-products of processing fruits and greens and from cereals, LWT–Food Sci. Technol. 32 (8) (1999) 503–508.
[44] Y. Lario, E. Sendra, J. Garcıa-Pérez, C. Fuentes, E. Sayas-Barberá, J. Fernández-López, J.A. Perez-Alvarez, Preparation of high dietary fiber powder from lemon juice by-products, Innovat. Food Sci. Emerg. Technol. 5 (1) (2004) 113–117.
[45] K. Srikaeo, M.S. Rahman, Proton relaxation of waxy and non-waxy rice by low field nuclear magnetic resonance (LF-NMR) to their glassy and rubbery states, J. Cereal. Sci. 82 (2018) 94–98.
[46] T. Li, X. Rui, C. Tu, W. Li, K. Wang, L. Huang, M. Dong, NMR Relaxometry and imaging to study water dynamics during soaking and blanching of soybean, Int. J. Food Eng. 12 (2) (2016) 181–188.
[47] S. Suresh, N. Guizani, M. Al-Ruzeiki, A. Al-Hadhrami, H. Al-Dohani, I. Al-Kindi, M.S. Rahman, Thermal characteristics, chemical composition and polyphenol contents of date-pits powder, J. Food Eng. 119 (3) (2013) 668–679.
[48] W. Rivera, X. Velasco, C. Gálvez, C. Rincón, A. Rosales, P. Arango, Effect of the roasting process on glass transition and phase transition of Colombian Arabic coffee beans, Procedia Food Science 1 (2011) 385–390.
[49] L.E. Kurozawa, I. Terng, M.D. Hubinger, K.J. Park, Ascorbic acid degradation of papaya during drying: effect of process conditions and glass transition phenomenon, J. Food Eng. 123 (2014) 157–164.
[50] W. Cao, Y. Nishiyama, S. Koide, Physicochemical, mechanical and thermal properties of brown rice grain with various moisture contents, Int. J. Food Sci. Technol. 39 (9) (2004) 899–906.
[51] M.S. Rahman, M.K. Al-Khusaibi, K.A. AL-Farsi, I.M. Al-Bulushi, A. Abushelaibi, N. Al-Habsi, Moisture sorption isotherm and thermal characteristics of freeze-dried tuna, International Journal of Food Studies 8 (1) (2019) 87–96.
[52] V. Orlien, J. Risbo, M. Andersen, L. Skibsted, The question of high- or low-temperature glass transition in frozen fish: construction of the supplemented state diagram for tuna muscle by differential scanning calorimetry, J. Agric. Food Chem. 51 (1) (2003) 211–217.
[53] R.G.M. Van der Sman, Progress in understanding of supplemented state diagrams of hydrophilic food materials, Curr. Opin. Food Sci. 21 (2018) 32–38.
[54] G.B. Sperandio, E.X. Filho, An overview of *Trichoderma reesei* co-cultures for the production of lignocellulolytic enzymes, Appl. Microbiol. Biotechnol. 105 (8) (2021) 3019–3025.
[55] S.R. Alyileili, K. El-Tarabily, W.H. Ibrahim, M. Sulaiman, A.S. Hussein, Effect of *Trichoderma reesei* degraded date pits supplementation on growth performance, immunoglobulin levels, and intestinal barrier functions of broiler chickens, Recent Pat. Food, Nutr. Agric. 11 (2) (2020) 168–181.
[56] R.S. Orozco, P.B. Hernández, G.R. Morales, F.U. Núñez, J.O. Villafuerte, V.L. Lugo, P.C. Vázquez, Characterization of lignocellulosic fruit waste as an alternative feed stock for bioethanol production, Bioresources 9 (2) (2014) 1873–1885.
[57] I. Sohail, S. Peerzada, N. Shehzadi, K. Hussain, M. Salman, R. Sher, M. Islam, Physicochemical and spectroscopic profiles for identification of seed (pits) of *phoenix sylvestris roxb*, Pakistan Journal of Pharmacy 29 (1) (2018) 20–26.
[58] I.I.B. Sharfan, K. Norrman, M.A. Abdulhamid, Thermal transformation of date seeds from nonporous to porous materials: Insights on structural changes using chemical and physical characterization, J. Anal. Appl. Pyrol. 177 (2024) 1–12 (Article 106353).
[59] H. Zhang, J. Wu, J. Zhang, J. He, 1-Allyl-3-methylimidazolium chloride room temperature ionic liquid: a new and powerful nonderivatizing solvent for cellulose, Macromolecules 38 (2005) 8272–8277.

[60] M. Zhong, J. Li, L. Zhou, T. Wang, J. Liu, M. Mei, S. Chen, Co-pyrolysis of cellulose and polyethylene terephthalate by TG-MS: Pyrolysis behavior, conventional gas and solid phase product characteristics, J. Anal. Appl. Pyrol. 172 (2023) 1–10 (Article 106002).
[61] J.X. Sun, X.F. Sun, H. Zhao, R.C. Sun, Isolation and characterization of cellulose from sugarcane bagasse, Polym. Degrad. Stabil. 84 (2) (2004) 331–339.
[62] N. Byrne, R. De Silva, Y. Ma, H. Sixta, M. Hummel, Enhanced stabilization of cellulose-lignin hybrid filaments for carbon fiber production, Cellulose 25 (1) (2018) 723–733.
[63] R. Miranda, D. Bustos-Martinez, C.S. Blanco, M.G. Villarreal, M.R. Cantu, Pyrolysis of sweet orange (*Citrus sinensis*) dry peel, J. Anal. Appl. Pyrol. 86 (2) (2009) 245–251.
[64] V. Hernández-Montoya, M.A. Montes-Morán, M.P. Elizalde-González, Study of the thermal degradation of citrus seeds, Biomass Bioenergy 33 (9) (2009) 1295–1299.
[65] R.C. Sun, X.F. Sun, J. Tomkinson, Hemicellulose and their derivatives, ACS (Am. Chem. Soc.) Symp. Ser. 864 (2004) 2–22.
[66] I. Pastorova, R.E. Botto, P.W. Arisz, J.J. Boon, Cellulose char structure: a combined analytical Py-GC-MS, FTIR, and NMR study, Carbohydr. Res. 262 (1) (1994) 27–47.
[67] M.S. Izydorczyk, C.G. Biliaderis, Cereal arabinoxylans: advances in structure and physicochemical properties, Carbohydrate Polymers 28 (1) (1995) 33–48.
[68] J.K. Adewole, A.S. Sultan, A study on processing and chemical composition of date pit powder for application in enhanced oil recovery, Defect Diffusion Forum 353 (2014) 79–83.
[69] M. Shen, W. Weihao, L. Cao, Soluble dietary fibers from black soybean hulls: physical and enzymatic modification, structure, physical properties, and cholesterol binding capacity, J. Food Sci. 85 (6) (2020) 1668–1674.
[70] D. Mudgil, The interaction between insoluble and soluble fiber, in: R.A. Samaan (Ed.), Dietary Fiber for the Prevention of Cardiovascular Disease, Elsevier, 2017, pp. 35–59.
[71] E.A.R. Assirey, Nutritional composition of fruit of 10 date palm (*Phoenix dactylifera L.*) cultivars grown in Saudi Arabia, J. Taibah Univ. Sci. 9 (1) (2015) 75–79.
[72] W. Lai, Using dietary fiber in food product development, Food Technol. 77 (3) (2023) 45–47.
[73] J.F. Douglas, Weak and strong gels and the emergence of the amorphous solid state, Gels 4 (2018) 1–14 (Article 19).
[74] K. Horie, M. Baron, R.B. Fox, J. He, M. Hess, J. Kahovec, W.J. Work, Definitions of terms relating to reactions of polymers and to functional polymeric materials, Pure Appl. Chem. 76 (4) (2004) 889–906.
[75] J. Vohlidal, Polymer degradation: a short review, Chemistry Teacher International 3 (2) (2020) 213–220.
[76] T.P. Shukla, Amorphous insoluble cellulosic fiber and method of making same US, Patent (2008) 1–9. US20080014325A1.
[77] B. Christ, W. Glaubitt, K. Berberich, T. Weigel, J. Probst, G. Sextl, S. Dembski, Sol-gel-derived fibers based on amorphous α-Hydroxy-Carboxylate-modified Titanium (IV) Oxide as a 3-dimensional scaffold, Materials 15 (8) (2022) 1–12 (Article 2752).
[78] M. Ranasinghe, N. Sivapragasam, H. Mostafa, I.O. Airouyuwa, I. Manikas, B. Sundarakani, S. Maqsood, C. Stathopoulos, Valorizing date seeds in biscuits: a novel approach to incorporate bioactive components extracted from date seeds using microwave-assisted extraction, Resources, Environment and Sustainability 15 (2024) 1–12 (Article 100147).
[79] D. Yankov, Fermentative lactic acid production from lignocellulosic feedstocks: from source to purified product, Front. Nutr. 10 (2022) 1–34 (Article 823005).